# Zooming in and out

Wang, Heng; van der Wal, Daphne; Li, Xiangyu; van Belzen, Jim; Herman, Peter M. J.; Hu, Zhan; Ge, Zhenming; Zhang, Liquan; Bouma, Tjeerd J.

*Published in:*
Journal of geophysical research-Earth surface

*DOI:*
10.1002/2016JF004193



*Publication date:*
2017

AGU PUBLICATIONS

JGR

Journal of Geophysical Research: Earth Surface

RESEARCH ARTICLE
10.1002/2016JF004193

**Key Points:**
- Retreat rate of the salt marsh edge is determined by factors acting at different spatial scales
- Sediment erodibility at the local scale is correlated with large-scale retreat rates of exposed sites lacking protective pioneer vegetation in front of the cliff
- Sediment grain size and root biomass significantly affect sediment erodibility

**Supporting Information:**
- Supporting Information S1

**Correspondence to:**
L. Zhang and T. J. Bouma,
lqzhang@sklec.ecnu.edu.cn;
tjeerd.bouma@nioz.nl

**Citation:**
Wang, H., D. van der Wal, X. Li, J. van Belzen, P. M. J. Herman, Z. Hu, Z. Ge, L. Zhang, and T. J. Bouma (2017), Zooming in and out: Scale dependence of extrinsic and intrinsic factors affecting salt marsh erosion, *J. Geophys. Res. Earth Surf.*, *122*, 1455–1470, doi:10.1002/2016JF004193.

Received 4 JAN 2017
Accepted 23 JUN 2017
Accepted article online 12 JUL 2017
Published online 29 JUL 2017



# Zooming in and out: Scale dependence of extrinsic and intrinsic factors affecting salt marsh erosion

**Heng Wang[1], Daphne van der Wal[2], Xiangyu Li[1], Jim van Belzen[2], Peter M. J. Herman[3], Zhan Hu[4], Zhenming Ge[1], Liquan Zhang[1], and Tjeerd J. Bouma[2,5]**

[1]State Key Laboratory of Estuarine and Coastal Research, East China Normal University, Shanghai, China, [2]Department of Estuarine and Delta Systems, NIOZ Royal Netherlands Institute for Sea Research and Utrecht University, Yerseke, The Netherlands, [3]Deltares, Delft, The Netherlands, [4]Institute of Estuarine and Coastal Research, School of Marine Science, Sun Yat-sen University, Guangzhou, China, [5]Community & Conservation Ecology, Faculty of Science and Engineering, University of Groningen, The Netherlands

**Abstract** Salt marshes are valuable ecosystems that provide important ecosystem services. Given the global scale of marsh loss due to climate change and coastal squeeze, there is a pressing need to identify the critical extrinsic (wind exposure and foreshore morphology) and intrinsic factors (soil and vegetation properties) affecting the erosion of salt marsh edges. In this study, we quantified rates of cliff lateral retreat (i.e., the eroding edge of a salt marsh plateau) using a time series of aerial photographs taken over four salt marsh sites in the Westerschelde estuary, the Netherlands. In addition, we experimentally quantified the erodibility of sediment cores collected from the marsh edge of these four marshes using wave tanks. Our results revealed the following: (i) at the large scale, wind exposure and the presence of pioneer vegetation in front of the cliff were the key factors governing cliff retreat rates; (ii) at the intermediate scale, foreshore morphology was partially related to cliff retreat; (iii) at the local scale, the erodibility of the sediment itself at the marsh edge played a large role in determining the cliff retreat rate; and (iv) at the mesocosm scale, cliff erodibility was determined by soil properties and belowground root biomass. Thus, both extrinsic and intrinsic factors determined the fate of the salt marsh but at different scales. Our study highlights the importance of understanding the scale dependence of the factors driving the evolution of salt marsh landscapes.

## 1. Introduction

Salt marshes are the higher areas of intertidal zones covered by halophytes, providing valuable ecosystem services and including habitats to support biodiversity, primary production, water purification, carbon sequestration, and coastal protection [*Craft et al.*, 2008; *Fourqurean et al.*, 2012; *Bouma et al.*, 2014]. However, salt marshes are confronted by two major threats, sea level rise, and coastal squeeze. Coastal squeeze [*Gedan et al.*, 2009; *Doody*, 2013] occurs when seawalls are built to prevent marshes from migrating landward as sea level rises [*Winn et al.*, 2003; *Allen*, 2002; *Feagin et al.*, 2009; *van de Koppel et al.*, 2005; *Francalanci et al.*, 2013]. Because of climate change [*Solomon*, 2007], sea levels are rising at increasing rates worldwide, which may lead to higher frequency of extreme events and subsequent marsh lateral erosion [*Craft et al.*, 2008; *Feagin et al.*, 2009; *Clough et al.*, 2010; *Mariotti et al.*, 2010; *Fagherazzi et al.*, 2013]. Several modeling studies have indicated that sea level rise may increase the risk of marsh edge erosion [*Mariotti and Fagherazzi*, 2010; *Marani et al.*, 2011; *Wang et al.*, 2014]. Moreover, recent studies have demonstrated that marsh edge erosion can occur even in the absence of sea level rise when the sediment supply is insufficient [*Fagherazzi et al.*, 2013; *Mariotti and Fagherazzi*, 2013]. Salt marshes, thus, are at risk from a combination of these stressors. Understanding the mechanisms responsible for marsh stability or deterioration in the face of climate change and sea level rise therefore is a key issue for salt marsh ecosystem protection and restoration.

In many eroding marshes, a pronounced salt marsh cliff forms at the edge of the marsh plateau facing the tidal flat. The essential process behind marsh edge erosion is wave-induced sediment surface erosion and mass collapse [*Marani et al.*, 2011; *Francalanci et al.*, 2013; *Tonelli et al.*, 2010]. "Surface erosion" is the gradual erosion of a small amount of particle at the vertical surface, akin the erosion process that occurs on a horizontal bed caused by the bed shear stress. "Mass failure" is the discontinuous release of large amounts of sediment by detachment of large blocks, starting with the tension cracks from the top of the marsh platform [*Francalanci et al.*, 2013]. These physical processes are influenced by a series of factors that are

extrinsic to the sediment properties, which regulate the erosivity of the waves, as well as intrinsic factors, which regulate the resistance of the cliff to being undermined by the force exerted by waves. Regarding the extrinsic factors, attacks by wind-driven waves are considered the dominant force driving the erosion process, among other physical processes such as long-shore currents and tidal action [*Schwimmer*, 2001]. Wave energy is a function of effective fetch [*Young and Verhagen*, 1996a, 1996b]. The erosion rate of the marsh edge is positively related to wave power density, which is a function of wind forcing [*Schwimmer*, 2001; *Marani et al.*, 2011] and, thus, also depends on the orientation of the marsh edge relative to the (pre) dominant wind direction [*Rubegni et al.*, 2013]. Indeed, *Marani et al.* [2011] found a linear relation between the density of the incident wave power and the retreat rate of the marsh edge. In addition, the presence of pioneer vegetation in front of the cliff can be considered an extrinsic factor because vegetation attenuates hydrodynamic energy before it reaches the salt marsh edge [*van de Koppel et al.*, 2005; *Yang et al.*, 2011; *Manca et al.*, 2012; *Möller et al.*, 2014]. Finally, the distance over which waves are dissipated across the tidal flat, and the shape (convexity/concavity) of the tidal flat, also affects the magnitude of wave energy reaching the cliff [*Hu et al.*, 2015]. Thus, foreshore morphology might also be an extrinsic factor affecting marsh edge erosion through attenuation of wave energy. In addition to extrinsic factors, the intrinsic resistance of the sediment may affect the stability of the marsh. Sediment and salt marsh vegetation properties have been shown to influence the stability of marsh cliffs in laboratory wave tank experiments [*Feagin et al.*, 2009; *Francalanci et al.*, 2013]. Using such experiments, *Feagin et al.* [2009] found that soil type is the primary variable influencing the lateral erosion rate and that plants only indirectly modify erodibility by modifying soil parameters.

Although these extrinsic and intrinsic factors have all been identified in previous studies, the effects of both types of factors on marsh edge erosion have rarely been quantified. Our study aimed to bridge these studies in order to quantify and assess the net effect of the main factor(s) at four different scales. We zoomed in from salt marshes at the level of the estuary (the large scale) to the mesocosm scale by combining analysis of salt marsh aerial photographs using geographic information system (GIS) with a wave tank experiment using sediment cores sampled from salt marsh edges. We explored the factors influencing wave erosivity (extrinsic) and sediment erodibility (intrinsic). Wave erosivity was studied indirectly by quantifying wind exposure, the presence/absence of pioneer vegetation in front of the cliff, and foreshore morphology. We addressed the following questions in this study: (1) What is the main factor affecting marsh edge erosion at each of the different spatial scales? (2) At which scales do the intrinsic factors affect marsh edge erosion? (3) What is the effect of sediment erodibility on the lateral retreat rate of salt marsh cliffs? Our findings were discussed in the light of implications for coastal management.

## 2. Materials and Methods

### 2.1. Study Area

The study area comprises four salt marshes located along the banks of the Westerschelde estuary (51.4°N, 4°E; Figure 1a), which has turbid, well-mixed waters and is a busy corridor for shipping. We selected four marsh sites with typical terrace-like marsh edges, stretching from midestuary in the east to the mouth of the estuary in the west: Zuidgors (Figure 1b), Waarde (Figure 1c), Paulina (Figure 1d), and Hellegat (Figure 1e). The spring tidal range varies from 5.5 m at the most eastward site (in the upper estuary) to 4.4 m at the most westward site (in the lower estuary). Waves are generally wind-generated, and the average significant wave height varies from about 0.1 m in the landward part of the basin to 0.4 m near the mouth [*Callaghan et al.*, 2010; *van der Wal et al.*, 2008]. Vegetation at the edge of marsh plateau in the study area includes *Spartina anglica*, *Aster tripolium*, *Atriplex portulacoides*, and *Elytrigia atherica*. We selected these four salt marsh sites based on their contrasting properties: we included two "exposed sites" Zuidgors and Waarde (Figures 1b and 1c) that are exposed to the predominantly southwestern wind in the Netherlands and two "sheltered sites" Paulina and Hellegat (Figures 1d and 1e). Within one marsh, different species can be found at the edge of the marsh plateau, and in front of this plateau, pioneer vegetation, *Spartina anglica*, can be present or absent. We distinguished 11 unique stretches (Figure 1; see Table 1 for an overview of the characteristics of these stretches). We further classified these 11 cliff stretches into four groups (Table 1). Using wind exposure (exposed or sheltered) and presence/absence of pioneer vegetation (with pioneer vegetation or bare flats in front of the cliffs), the four following groups were defined: exposed cliffs with pioneer vegetation in front (exposed-pioneer cliffs), exposed cliffs

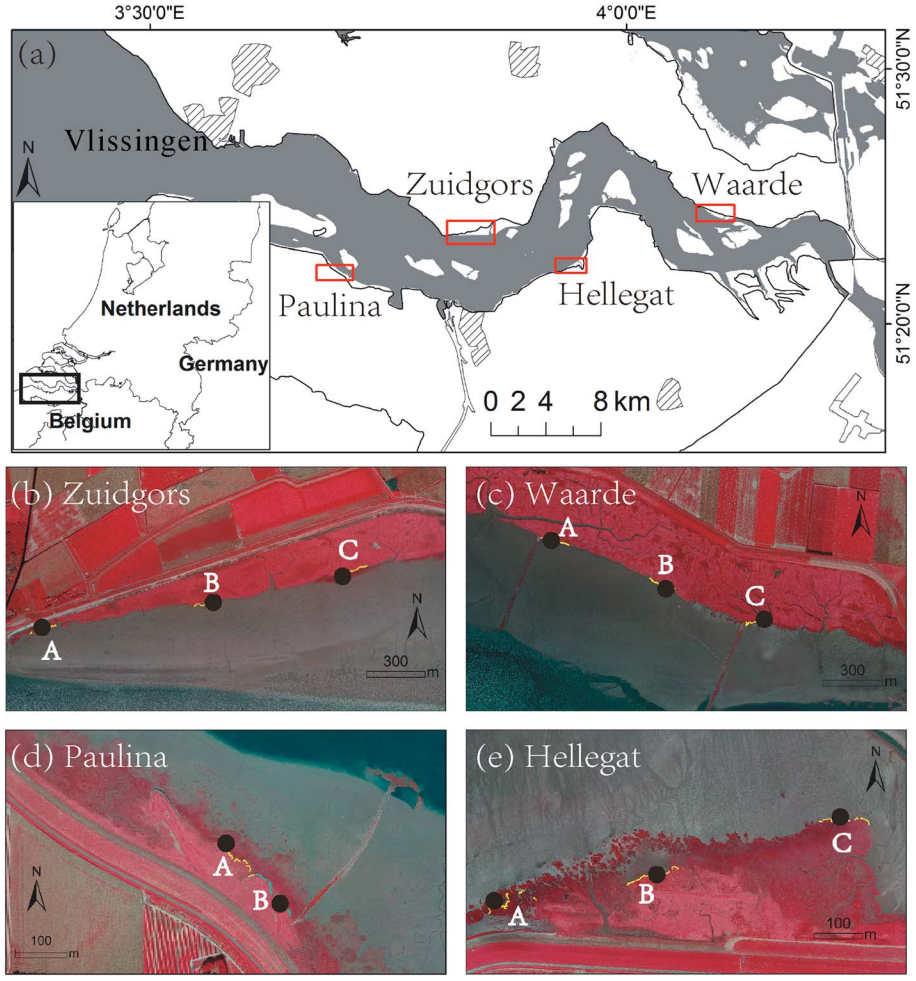


**Figure 1.** (a) Location of the salt marsh sites in the Westerschelde estuary, southwest Netherlands: (b) Zuidgors, (c) Waarde, (d) Paulina, and (e) Hellegat. Stretches within the sites are indicated with capital letters.

without pioneer vegetation (exposed-bare cliffs), sheltered cliffs with pioneer vegetation (sheltered-pioneer cliffs), and sheltered cliffs without pioneer vegetation (sheltered-bare cliffs).

### 2.2. GIS Analyses of Aerial Photographs and Digital Elevation Model

#### 2.2.1. Erosion Rate of the Marsh Edge (Cliff Lateral Retreat Rate)

The rate of marsh edge erosion was quantified as the rate at which the cliff retreated landward, which can be measured from high-resolution aerial photographs and digital elevation models (DEMs). Sequential false

**Table 1.** Characteristics of Stretches in the Study Area

| Site | Stretch | Exposed /Sheltered to SW Wind | Pioneer Condition | Salt Marsh Species |
|---|---|---|---|---|
| Hellegat | A | Sheltered | Pioneer vegetation | *Spartina anglica* |
| | B | Sheltered | Pioneer vegetation | *Atriplex portulacoides* |
| | C | Sheltered | Bare flat | *Spartina anglica* |
| Paulina | A | Sheltered | Pioneer vegetation | *Elytrigia atherica* |
| | B | Sheltered | Pioneer vegetation | *Elytrigia atherica* |
| Waarde | A | Exposed | Bare flat | *Aster tripolium* |
| | B | Exposed | Bare flat | *Elytrigia atherica* |
| | C | Exposed | Pioneer vegetation | *Elytrigia atherica* |
| Zuidgors | A | Exposed | Bare flat | *Atriplex portulacides* |
| | B | Exposed | Bare flat | *Elytrigia atherica* |
| | C | Exposed | Pioneer vegetation | *Elytrigia atherica* |

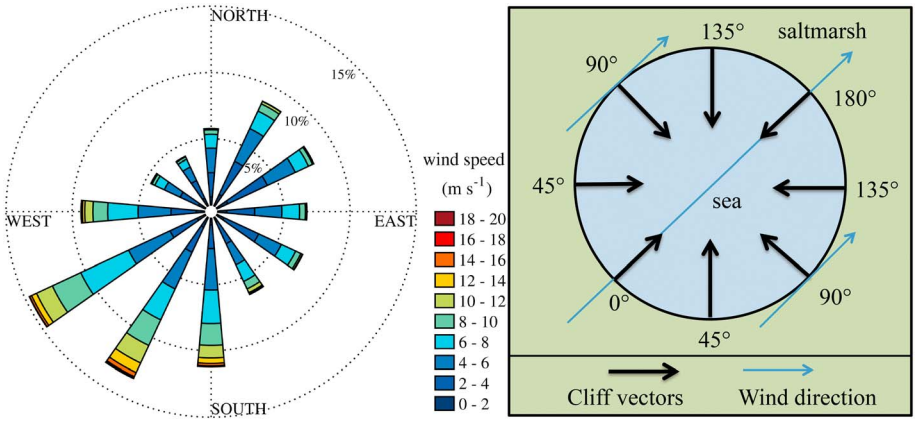


**Figure 2.** (a) Wind roses for 1971–2000. The concentric circles with percentages represent the wind frequencies. Data were acquired from the weather station at Vlissingen, the Netherlands. (KNMI, the Royal Dutch Meteorologial Institute) http://www.knmi.nl/samenw/hydra/cgi-bin/freqtab.cgi. (b) Definition of cliff wind exposure (WE). Cliff vectors were formed by adjacent pairs of cliff points, pointing from the marsh to the sea. The angle formed between the SW wind, and the cliff vector was defined as the wind exposure along the terrestrial–marine boundary.

color aerial photographs from the years 2008 and 2012 were used in this study, with a spatial resolution of 0.25 m by 0.25 m. The polylines of the salt marsh edge were traced in ArcGIS 10.3. During digitization, the scale was always kept at 1:400 to ensure an identical tracing resolution. The cliff polyline of 2012 was dotted every 3 m using MATLAB, and bisectors of the angles formed with three adjacent points on the 2012 cliff line were made. The bisectors were intersected with the cliff polyline of 2008. The distance of cliff lateral movement was quantified as the difference between the position of each cliff point in 2012 and the corresponding intersections in 2008. The mean rate of marsh edge retreat was defined as the retreat distance per year. Note that the retreat rate of the exposed-bare marsh edge that we obtained during the study period is comparable to the rate of salt marsh plateau retreat at the same marsh site Zuidgors during the period between 1982 and 2004, when more than 100 m marsh was eroded [*van der Wal et al.*, 2008]. Even though calculating the mean retreat rate based on aerial photographs only 4 years apart may seem limited in power, the relatively low variability indicates that it is a suitable proxy for the rate of marsh edge erosion. Moreover, this method ensures that the distance of cliff retreat is quantified in a spatially even manner. Since the error of tracing cliff points is caused by cell size, the maximum error is 0.25 m and the error of retreat rate is less than this at 0.125 m/yr (0.5 m/4 years).

#### 2.2.2. Wind Exposure and Wave Height

Based on pairs of adjacent cliff points, cliff wind exposure was defined by the angle between each cliff vector (pointing to the sea) and the predominant wind direction, which is southwesterly in the study area. Both frequency and magnitude are much higher than winds from other directions (Figure 2a). Defined as such, the wind exposure (WE) ranged from 0 to 180° (Figure 2b). At exposed salt marsh sites, WE ranges from 90 to 180°, and at sheltered cliffs, WE ranges from 0 to 90°. *van der Wal et al.* [2008] has already shown that Zuidgors (86.83%) experiences a much higher frequency of high-magnitude onshore winds than Hellegat (7.14%) and Paulina (2.88%).

The Simulating WAves Nearshore [SWAN, *Booij et al.*, 1999; *Ris et al.*, 1999] two-dimensional model was used to simulate wavefield under the predominant wind (SW). The model grid was located over the Westerschelde estuary from the North Sea to 110 km upstream with increments of 180 m. Since our main objective was to obtain a simple relation between wind exposure and wave height, the model was only forced by a constant and uniform wind (7 m/s), without the tidal effects on water depth or current. The bathymetry of 2013 is expressed in centimeter relative to Normaal Amsterdams Peil (NAP) (i.e., the Dutch ordnance level, similar to mean sea level), with 20 m resolution, obtained from Rijkswaterstaat that was used in the simulation. The longshore wave height was extracted. A linear regression was established of wave height as a function of wind exposure for the whole estuary.

#### 2.2.3. Foreshore Morphology

Quantification of foreshore morphology was based on digital elevation models (DEMs) from 2012 obtained from Rijkswaterstaat, with 20 m resolution. DEM data are expressed in m above NAP, and data were

projected to the Dutch national grid (Rijksdriehoekstelsel (RD)). At first, tidal levels of mean water level (MWL), mean low water level (MLWL) contour lines of mean low water level, were extracted from the DEMs. In this study, the width and slope of the mudflat and the width of the navigation channel were included in the foreshore morphology parameters. The width of the mudflat and the channel together approximately equals the estuary width. Because of the contrasting water depths of these two sections, we quantified them separately instead of together with the estuary width. For the width of the mudflat (m), we measured the direction perpendicular to the trend of marsh boundary at each site. Multiple lines were traced from each 2012 cliff point and intersected with contour lines. Width of the mudflat (m) was defined as the distance from the cliff to MLWL along the direction perpendicular to the cliff. Channels were defined as areas below MLWL. The width of the channel (m) was the distance between two MLWLs along the direction perpendicular to the cliff. The slope of the mudflat (degrees) was defined as the arctangent of the ratio between the vertical difference in elevation (m) of MWL and MLWL, and the horizontal distance (m) between MWL and MLWL.

#### 2.2.4. Sedimentation Rate

The mudflat elevations (m, above NAP) of Zuidgors were extracted from both the DEM of 2012 and 2013, projected in RD. In front of each cliff stretch (A, B, and C) of Zuidgors, 10 transects, with 10 points (interval: 20 m) in each, were made to extract the value of elevation in ArcGIS 10.3. The span of the elevation measurement across and alongshore were both 200 m. The net sedimentation rate (m/yr) was defined as the difference of elevation between 2012 and 2013. The average and standard error of sedimentation rates of 10 points at the same distance away from the cliff were calculated. The sediment rates should be interpreted with some caution, as the bathymetry may not always only represent the sediment surface, as this may be obscured by the vegetation.

### 2.3. Sediment Analyses and Wave Tank Experiment

#### 2.3.1. Sample Collection

Four replicates of mud samples were extracted from each of the stretches using PVC pipes (height = 30 cm, diameter = 15 cm). PVC pipes were inserted into the marsh surface vertically to avoid sample compaction and extracted with the intact sediment sample after digging around the core. The sediment core and attached plants were transferred from the PVC pipes to a cylindrical metal core (height = 30 cm, diameter = 15 cm) with an opening (width = 12 cm) on the longitudinal side, through which sediment could be exposed to waves in a wave tank (Figure 3c). The height of the sediment in the metal cores was 15 cm.

#### 2.3.2. Sediment Properties

Another four replicate sediment samples were collected at each marsh stretch to measure sediment properties, using a syringe from which the tip was cut off. The sediment and roots sticking out of the syringe were cut off. Each sediment sample (20 $cm^3$) was placed in a preweighed sample bottle and then placed in the freezer for 3 days. The bottles were then opened and placed into a freeze dryer (Christ® Alpha 1-4) until the air pressure inside the chamber had decreased below 0.06 bar. Samples were reweighed with the bottle after the samples had cooled down to room temperature. Bulk density of the sediment (in $g/cm^3$) was calculated as the ratio of the dry weight of the sediment sample to its volume. The sediment particle size distribution was determined by laser diffraction (Malvern Mastersizer 2000), from which the median grain size of the sediment $D_{50}$ (μm) was derived.

#### 2.3.3. Sediment Erodibility From Wave Tank Experiments

Since marsh edge erosion is affected by many extrinsic factors in the field, to eliminate the effects of extrinsic factors and explore the erodibility (the intrinsic property) of the marsh edge, sediment samples were subjected to identical wave force in the wave tank experiments, simulating the vertical erosion process of surface erosion in the field. Due to the limited scale of the sediment cores (diamater = 15 cm), simulation of mass wasting processes was not realistic. To quantify sediment erodibility, we measured the difference of sediment volume between the time steps under wave scouring. Twelve sediment cores were placed randomly into each of four tanks with three slots in each tank (length 2.76 m, width 0.9 m, and depth 0.79 m). Waves were generated by pistons at the other end of the wave tanks. Paddle movement was driven by the pistons when the air pressure reached 8 bar. The averaged wave height and wave frequency were 18 cm and ~0.5 Hz, respectively, which are comparable to the measured significant wave heights during windy weather at the salt marsh sites (Zuidgors: 23 ± 7 cm, Paulina: 19 ± 8 cm, and Hellegat: 18 ± 11 cm) [*Callaghan et al.*, 2010]. Water depth was 0.19 m in the wave tanks, which was 0.01 m above the base of the cores.

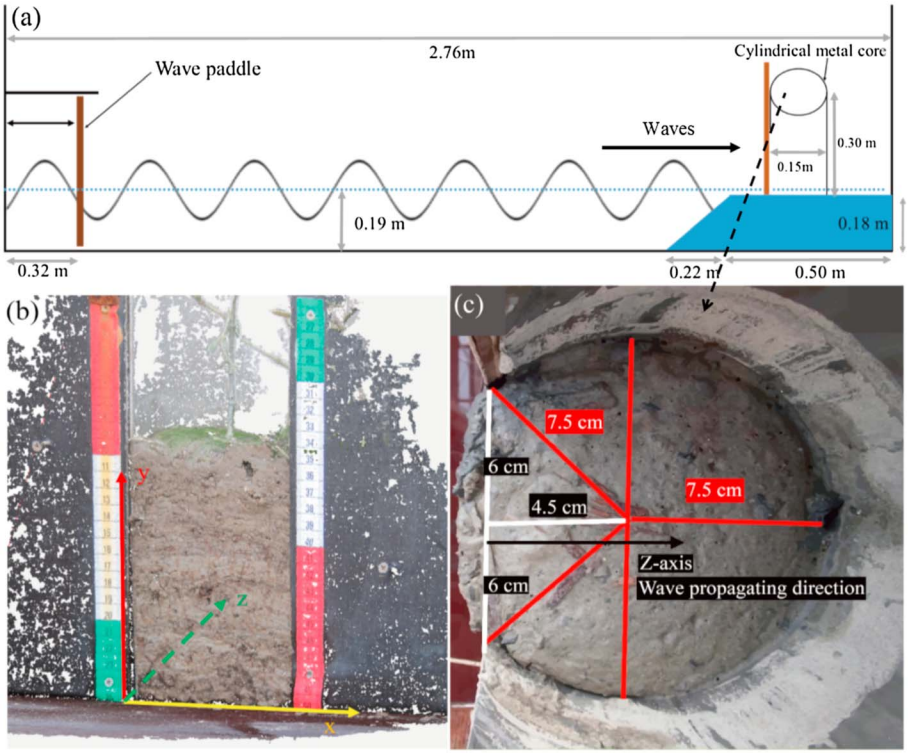


**Figure 3.** (a) A schematic side view of the wave tank used to measure cliff erosion rates in the laboratory. (b) Threedimensional representation of sediment core with right-handed *x*, *y*, and *z* coordinates building in Visual SFM. (c) The top view of each single sediment core.

We used a photogrammetry technique (structure from motion) [*Nieuwhof et al.*, 2015] to quantify the volume being eroded. At each time step, at least 40 photos were taken of each core. Photos were taken at 10 time steps (start, 1 h, 2 h, 4 h, 8 h, 16 h, 24 h, 32 h, 40 h, and 48 h) in a single run. With the open source software Visual SFM, three-dimensional representations of the sediment surface were produced as a set of data points with *x*, *y*, and *z* coordinates (Figure 3b). This point cloud was georeferenced using three control points (1 h; Figure 4a). Root-mean-square error was lower than 0.003 m during the georeferencing in Visual SFM. Then the point cloud was rasterized in MATLAB to a resolution of 0.003 m per raster pixel in order to allow for volume loss calculations. Volume loss at one time step was calculated as the difference in distance along the *z* plane of each raster pixel from the initial condition using MATLAB (Figure 3b). To eliminate the effects of optical reflection in the water, the volume loss was calculated within a window above the still water level with *x* coordinates ranging from 1 to 11 cm and *y* coordinates ranging from 2 to 14 cm (Figure 4). Thus, the area of the front frame was constant (10 cm * 12 cm = 120 $cm^2$).

$$\text{Volumeloss}_i = A^* \sum_{k=1}^{n} \left(z_i^k - z_0^k\right)$$

where *A* is the area of the window, *n* is the number of pixels, and *i* is the time step.

The volume loss of each sediment core at all time steps was then fitted with logarithmic, exponential, and linear functions; the $R^2$ of the logarithmic function was the highest among these three types of fitted functions. Generally, the sediment eroded the mostly quickly at the beginning of wave scouring. Therefore, the derivative at the end of the first experimental period ($t$ = 1 h) was used as a proxy for the rate of sediment volume loss ($cm^3$/h) (Table S1 in the supporting information), because at this time step, the loose sediment at the vertical surface caused by front cutting was removed by a 1 h wave attack. The average erosion rate of four replicates was used to experimentally quantify the marsh cliff erodibility. Compared with weighing methods, this volume loss method avoids deforming the sediment cores by handling (i.e., taking cores in and out of the wave tanks for each measurement) or weight errors arising from waterlogging of the cores.

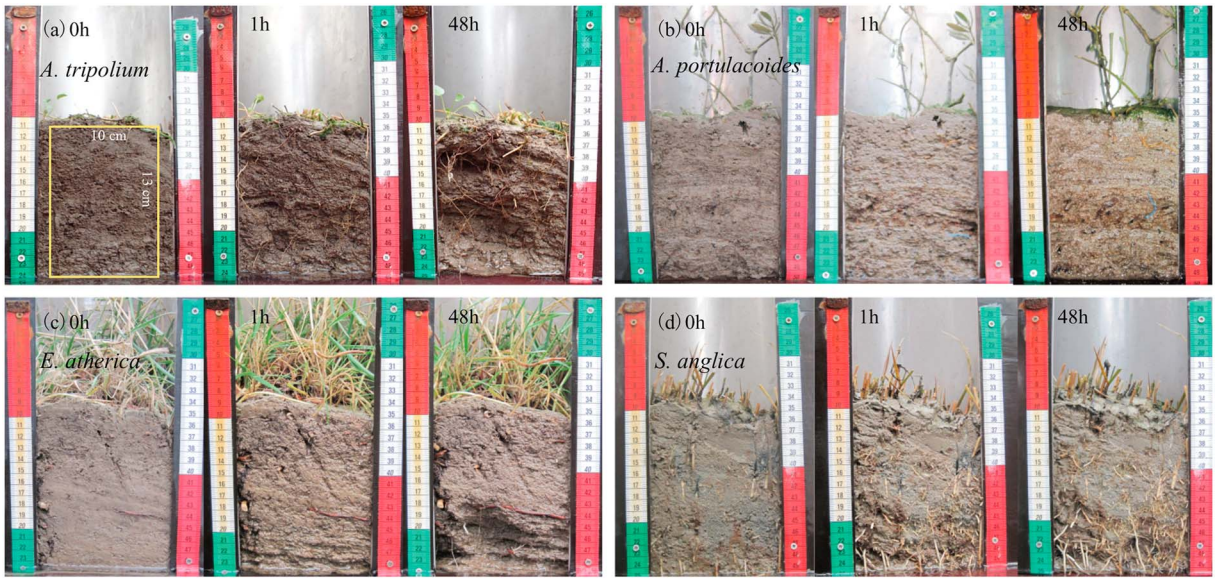


**Figure 4.** Photos of sediment cores at the initial time step, 1 h, and 48 h, with four species, (a) *Aster tripolium*, (b) *Atriplex portulacoides*, (c) *Elytrigia atherica*, and (d) *Spartina anglica*. To avoid errors due to water reflection at the lower sections of the cores, the volume loss of sediment was measured within the yellow frame (10 cm * 12 cm).

#### 2.3.4. Belowground Biomass of Vegetation

After the cores had been exposed for 48 h to the waves in the wave tanks, the remnant roots were carefully cleaned and washed in a 1 mm sieve to remove mud attached to roots. Each biomass sample was dried in an oven at 60°C until the weight was constant.

### 2.4. Statistical Data Analysis

In order to investigate the scale-dependent effects of factors on marsh boundary erosion, the data analyses were done at four spatial scales.

#### 2.4.1. Large Scale

This scale was defined as the edges of salt marshes in the whole Westerschelde estuary. Statistical data analysis was done including all point-specific data of four studied marshes. Linear regressions were performed to examine the relation between cliff wind exposure (degree) and lateral retreat rate (m/yr). Exposed and sheltered sites were tested separately to account for the effect of pioneer vegetation. Two-way analysis of variance (ANOVA) was used to test if there was a significant interaction between wind exposure and pioneer vegetation on cliff retreat.

#### 2.4.2. Intermediate Scale

Zooming into the intermediate scale, we tested which extrinsic factors (mudflat width, channel width, and mudflat slope) were important for cliff retreat within each of the four cliff groups (exposed-pioneer cliffs, exposed-bare cliffs, sheltered-pioneer cliffs, and sheltered-bare cliffs).To explore how foreshore morphology properties affected the cliff retreat rate, multiple linear regression was conducted at two scales, among all cliff points (large scale) and within groups with comparable hydrodynamic conditions (intermediate scale: within groups of exposed-pioneer, sheltered-pioneer, exposed-bare, and sheltered-bare stretches). ANOVA was used after multiple linear regression to identify the factors that contributed most to cliff retreat rate in the linear regression model.

#### 2.4.3. Local Scale

In order to test to what extent sediment erodibility affects marsh edge erosion at the local scale, correlation analyses were used to compare cliff lateral retreat rate and sediment volume loss rate, using data of all cliff stretches of four studied marshes and exposed-bare group, separately.

#### 2.4.4. Mesocosm Scale

To examine the effects of soil type and vegetation species on sediment volume loss rate, ANOVA was used to test for the effect of soil type and vegetation species, and the interactions between them, on cliff sediment volume loss rate.

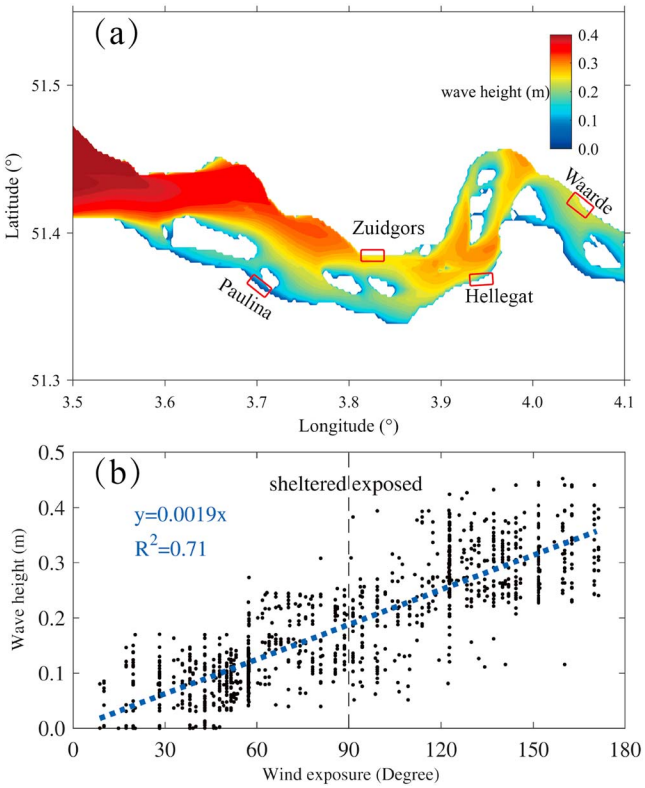


**Figure 5.** (a) Simulation of wave height by the wave generation and propagation model (SWAN). (b) Linear regression of shoreline wind exposure (degree) in the Westerschelde and the wave height (m) ($y = 0.0019x$, $R^2 = 0.71$).

All statistical analyses were run in R (an open-source language and environment for statistical computing, http://www.R-project.org). All tests were performed applying significance levels of $\alpha = 0.05$ (marked with *), 0.01 (marked with **), and 0.001(marked with ***).

## 3. Results

### 3.1. Large-Scale Effects of Wind Exposure and Pioneer Vegetation

The wave height in the Westerschelde estuary was generally decreasing from west to east under the SW wind (Figure 5a). The northern shoreline, exposed to the SW winds, was under higher wind wave force than the southern shoreline. The northwestern part of the estuary was exposed to wind waves with the highest wave height (>0.3 m). On the northern shoreline, wave at Zuidgors was slightly lower than at Waarde, the eastern marsh. On the contrary, the western marsh, Paulina was associated with the lower wave height than the eastern marsh Hellegat. The sheltered marsh Paulina was under limited wind waves (< 0.1 m). The wave height was linearly related the wind exposure ($y = 0.0017x$, $R^2 = 0.71$) in the Westerschelde estuary (Figure 5b).

Generally, cliffs with high exposure to wind (i.e., 90–180° to SW; Figure 6a) retreated faster than sheltered ones (i.e., 0–90° to SW; Figure 6a). Linear regressions between wind exposure and the retreat rate show that this relation is significant for cliffs without protective pioneer vegetation ($n = 819$, $R^2 = 0.4296$, ***) but not for cliffs with protective pioneer vegetation ($n = 706$, $R^2 = 0.0629$, ***) (Figure 6a and Table 2). Cliffs fronted by bare mudflats had a positive regression slope (slope = 0.0149). In contrast, the slope of cliffs with pioneer vegetation was −0.0026, very close to 0, which suggests that there was no significant linear relation among cliffs with pioneer vegetation, regardless of whether the cliffs were exposed or sheltered. The retreat rates of cliffs fronted by pioneer vegetation were statistically lower and rarely varied with wind exposure. The two-way ANOVA showed that this interaction between exposure and pioneer vegetation had a significant effect on cliff retreat rate ($p < 0.001$; Table 3). Even though both wind exposure and the presence of pioneer vegetation had significant main effects on marsh edge erosion rate, the presence of pioneer vegetation explained much more of the variation (higher sum of squares and mean square) than wind exposure ($p < 0.001$; Table 3).

Cliffs with pioneer vegetation on the mudflat in front of cliffs retreated more slowly than adjacent cliffs with bare tidal flats in front, regardless of cliff exposure to the SW wind (Figure 6b; boxes a and b versus c and d). In summary, taking all cliff points into consideration at the large scale, lateral retreat of salt marsh cliffs was significantly related to presence of pioneer vegetation, wind exposure, and their interaction effects.

### 3.2. Intermediate-Scale Effects of Foreshore Morphology

Multiple linear regression (Table 4) showed that in the exposed-pioneer and sheltered-pioneer cliff groups, cliff lateral retreat rate was significantly related to channel width ($p < 0.001$ in both groups) and mudflat

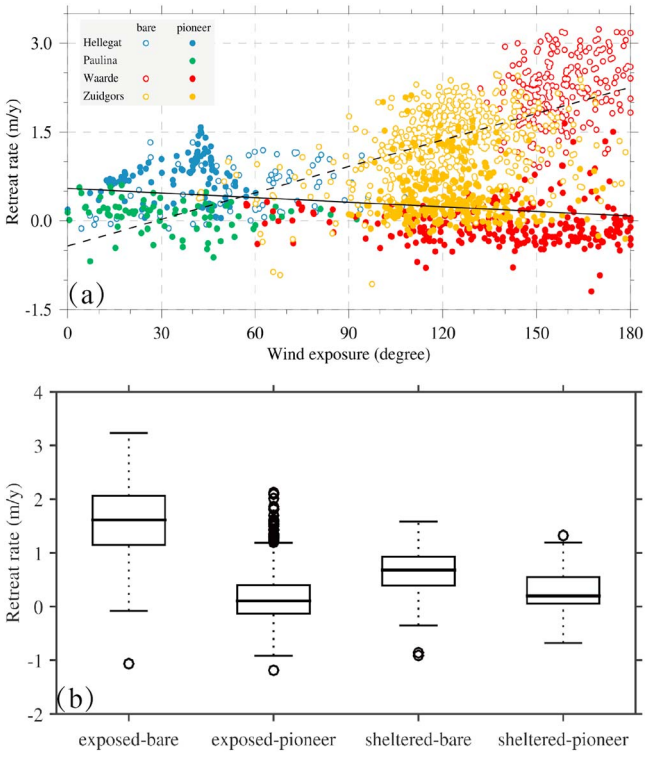


**Figure 6.** (a) Linear regressions between cliff wind exposure (degree) and cliff lateral retreat rate (m/yr), including cliff points of the four salt marsh sites Hellegat (pioneer and bare cliffs), Paulina (only pioneer cliffs), Waarde (pioneer and bare cliffs), and Zuidgors (pioneer and bare cliffs). The dashed line represents the linear regression between the retreat rate of cliffs without pioneer vegetation and wind exposure ($y = 0.0149x - 0.4221$), and the solid line represents the cliffs with pioneer vegetation in front ($y = -0.0026x + 0.5473$). (b) Boxplots of cliff lateral retreat rate in four class levels crossing wind exposure and presence of pioneer vegetation. The maximum, 75th percentile; median, 25th percentile; and minimum values are represented for each of the cliff groups. The open circles depict outliers.

slope ($p < 0.05$ in exposed-pioneer group and $p < 0.001$ in sheltered-pioneer group). Within these two pioneer groups, neither wind exposure ($p > 0.05$ in both groups) nor mudflat width ($p > 0.05$ in both groups) significantly affected cliff retreat. The linearly fitted cliff retreat rate based on the multiple regression model and the measured retreat rate were highly correlated, with a correlation coefficient $R^2 = 0.74$ for the exposed-pioneer group as a whole, $R^2 = 0.17$ for Waarde cliffs, and $R^2 = 0.56$ for Zuidgors cliffs (Figure 7a). For sheltered-pioneer cliffs, the measured retreat rate was also correlated with the fitted rate: $R^2 = 0.72$ for the whole group, $R^2 = 0.77$ for Hellegat, and $R^2 = 0.18$ for Paulina (Figure 7b).

In the exposed-bare and sheltered-bare cliff groups, lateral retreat rate of exposed-bare cliffs was linearly related to wind exposure ($p < 0.001$ in exposed-bare group and $p < 0.05$ in sheltered-bare group), mudflat width ($p < 0.001$ in both groups), and channel width ($p < 0.001$ in exposed-bare group and $p < 0.01$ in sheltered-bare group) but not mudflat slope. The linearly fitted cliff retreat rate of exposed-bare cliffs and the measured rate were highly correlated, with a correlation coefficient $R^2 = 0.78$ for the whole group, $R^2 = 0.47$ for Waarde cliffs, and $R^2 = 0.68$ for Zuidgors cliffs (Figure 7c). For sheltered-bare cliffs, which only included stretch C at Hellegat, measured retreat rate was still correlated with the fitted one ($R^2 = 0.90$; Figure 7d).

In both the pioneer and bare groups, the correlation coefficient of a single marsh site was lower than that of the whole group (Figures 7a–7c), and the slope between observed and fitted rates differed per site. This suggests that apart from the foreshore morphology factors we considered, additional factors that vary between sites might play a role in the dynamics of lateral marsh retreat.

**Table 2.** Linear Regressions Between Wind Exposure (Degree) and Lateral Retreat Rate (m/yr) of Cliffs With and Without Pioneer Vegetation[a]

| | Variables | Coefficient | Std. Error | *t* Value | $p$ (>$t$) | $R^2$ |
|---|---|---|---|---|---|---|
| Cliff without pioneer vegetation | (intercept) | −0.422 | 0.0783 | −5.391 | 9.19e-08*** | 0.74 |
| | exposure | 0.0149 | 0.0006 | 24.805 | < 2e-16*** | |
| Cliff with pioneer vegetation in front | (intercept) | 1.332 | 0.392 | 3.400 | <0.001*** | 0.72 |
| | exposure | 0.001 | 0.001 | 0.785 | 0.434 | |

[a]Std. Error = standard Error.
***$p < 0.001$.
**$p < 0.01$.

**Table 3.** Two-Way Analysis of Variance of Cliff Lateral Retreat Rate, Volume Loss Rate, and Belowground Biomass[a]

| Response Variable | Source of Deviance | d.f., *N* | Sum Sq | Mean Sq | *F* Value | *p* (>F) |
|---|---|---|---|---|---|---|
| Cliff lateral retreat rate (m/yr) | Exposure | 1, 1448 | 122.1 | 122.1 | 342.7 | <0.001*** |
| | Pioneer | 1, 1448 | 564.4 | 564.4 | 1584.2 | <0.001*** |
| | Exposure * pioneer | 1, 1448 | 64.7 | 64.7 | 181.6 | <0.001*** |
| Volume loss rate (cm/h) | Species | 1, 44 | 2524 | 841.5 | 5.55 | 0.00178** |
| | Soil type | 1, 44 | 2753 | 1376 | 9.413 | <0.001*** |
| | Species * soil type | 1, 44 | 808 | 808.3 | 8.115 | 0.00583** |
| Belowground biomass (g) | Species | 2, 44 | 3135.7 | 1567.8 | 20.54 | <0.001*** |

[a]d.f. = degree of freedom, Sum Sq = sum of squares, Mean Sq = mean of squares.
***$p < 0.001$.
**$p < 0.01$.

### 3.3. Local-Scale Effects of Sediment Erodibility

No significant linear relationship was found between the sediment volume loss rate (i.e., sediment erodibility) measured during the wave tank experiments and the rate of lateral cliff retreat (i.e., marsh edge erosion rate) derived from the aerial photographs ($R^2$ = 0.0191, $n$ = 11, $p$ = 0.685; Figure 8a). This suggests that other factors, as described in the previous sections, overruled the effects of intrinsic factors on cliff retreat rate.

Within the marsh Zuidgors, wind exposure along the shoreline was similar. The net sedimentation rate is significantly higher in the stretch with pioneer vegetation (Zuidgors-C) than in the bare stretches (Zuidgors-A and B) (Figure 8b). Accretion of the mudflat in front of the pioneer vegetation zone increased slightly seaward, while the accretion rate of Zuidgors-B decreased seaward. In contrast, the mudflat in front of stretch A eroded.

Eliminating the strong effects of pioneer vegetation and wind exposure on cliff lateral retreat rate in order to focus on subtler effects, we concentrated on the stretches of the exposed-bare group. Waarde and Zuidgors showed the same trend: stretches with high erodibility were accompanied by high marsh edge erosion rates within one marsh site. In the wave tank experiment, either in marsh Waarde or Zuidgors, the sediment volume loss rate of stretch B is higher than that of stretch A. In addition, the cliff retreat rate of stretch B is

**Table 4.** Multiple Linear Regression of Cliff Lateral Retreat Rate With Wind Exposure (Degree), Mudflat Width (m), Channel Width (m), and Mudflat Slope (Degree)[a]

| | Variables | Estimate | Std. Error | *t* Value | *p* (>t) |
|---|---|---|---|---|---|
| Exposed-pioneer | (intercept) | 0.003 | 0.198 | 0.013 | 0.990 |
| | WE | 0.000 | 0.001 | −0.035 | 0.972 |
| | Mudflat width | 0.001 | 0.000 | −0.180 | 0.857 |
| | Channel width | 0.001 | 0.000 | 4.723 | <0.001*** |
| | Mudflat slope | 0.184 | 0.086 | 2.134 | <0.05* |
| Sheltered-pioneer | (intercept) | 1.332 | 0.392 | 3.400 | <0.001*** |
| | WE | 0.001 | 0.001 | 0.785 | 0.434 |
| | Mudflat width | 0.001 | 0.001 | 0.110 | 0.913 |
| | Channel width | 0.002 | 0.000 | −3.522 | <0.001*** |
| | Mudflat slope | −0.514 | 0.136 | −3.785 | 0.000222*** |
| Exposed-bare | (intercept) | −0.308 | 0.364 | −0.848 | 0.397 |
| | WE | 0.006 | 0.001 | 7.222 | 1.28e-12*** |
| | Mudflat width | 0.002 | 0.000 | 4.585 | <0.001*** |
| | Channel width | 0.003 | 0.000 | −8.906 | <0.001*** |
| | Mudflat slope | 0.141 | 0.128 | 1.102 | 0.271 |
| Sheltered-bare | (intercept) | 0.400 | 0.577 | 0.694 | 0.490 |
| | WE | 0.003 | 0.002 | 1.991 | 0.050 |
| | Mudflat width | 0.004 | 0.001 | 5.855 | <0.001*** |
| | Channel width | 0.008 | 0.003 | −2.737 | <0.01** |
| | Mudflat slope | 0.053 | 0.085 | 0.630 | 0.530 |

[a]WE = wind exposure.
***$p < 0.001$.
**$p < 0.01$.
*$p < 0.05$.

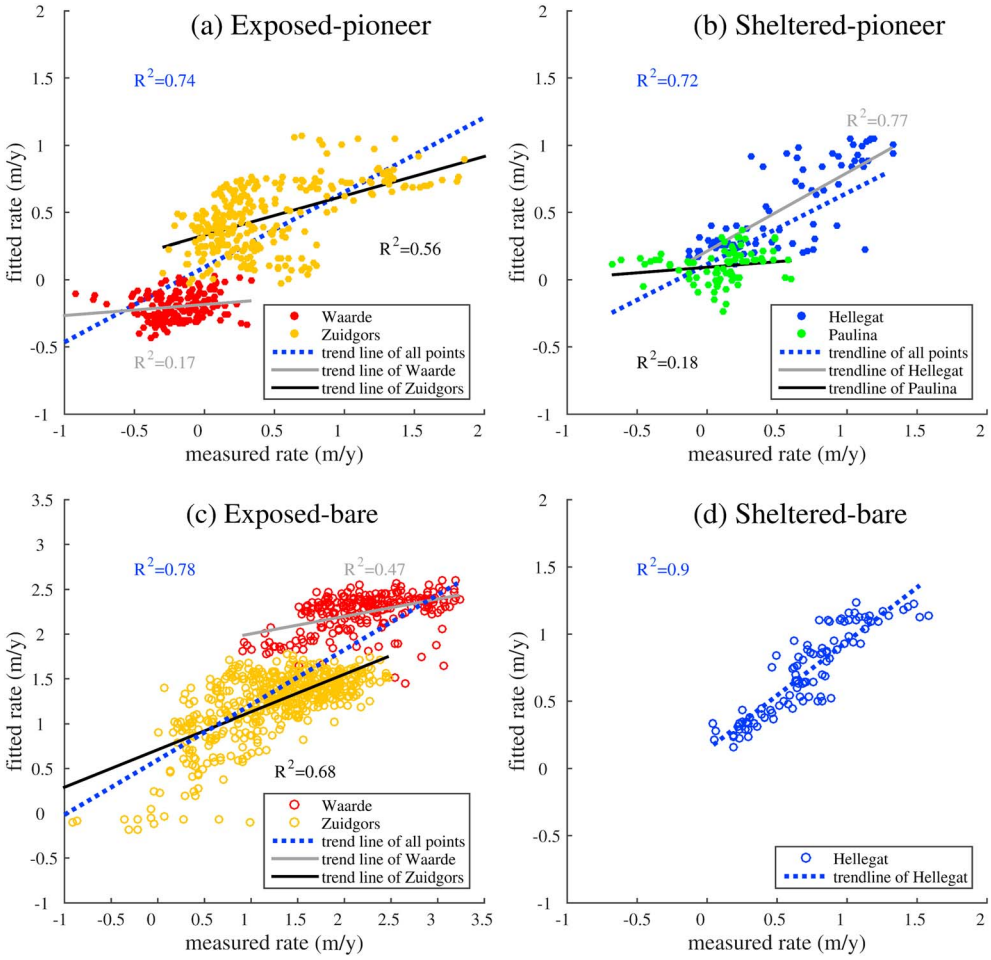


**Figure 7.** Correlations between multiple linear fitted lateral retreat rates and measured retreat rates with four types of foreshore conditions: (a) exposed-pioneer, (b) sheltered-pioneer, (c) exposed-bare, and (d) sheltered-bare stretches. The blue dashed lines represent the trend lines of each group. The black and solid grey lines represent the trend lines of stretches within each group. The colors of the $R^2$ text match the color of its corresponding trend line.

more rapidly than stretch A (Figure 8c). For Waarde, the correlation is stronger than for Zuidgors. The observed cliff retreat rate for Waarde A and B is significantly faster than for Zuidgors A and B. Thus, the sediment volume loss rate corresponded to the rate of cliff lateral retreat for the exposed-bare cliffs of Waarde and Zuidgors, suggesting that the erodibility of the cliffs played a large role in the local cliff retreat rates within bare stretches with similar wind exposure (Waarde: 157 ± 10.71°; Zuidgors: 121.77 ± 21.14°).

### 3.4. Mesocosm-Scale Effects of Sediment and Vegetation on Sediment Erodibility

The mean sediment grain size of exposed cliffs was less than 50 μm, finer than that for sheltered cliffs (Figure 9a). Moreover, sediment volume loss rates differed significantly between the four plant species ($p < 0.05$; Table 3). In addition, the effect of sediment grain size on sediment erodibility was highly significant ($p < 0.001$; Table 3 and Figure 9a) and the effects of plant species and sediment grain size were not independent of each other but interacted on sediment erodibility ($p < 0.05$; Table 3).

Sediment volume loss rate (Table S1) was inversely related to the root biomass of each sediment sample and could be fitted with an inverse function (Figure 9b). Generally, samples with a smaller amount of root biomass were associated with sediment eroding more rapidly at the beginning of the wave thrust. In our samples, significant differences in root biomass were found between plant species ($p < 0.001$; Table 3). Sediment samples with *E. atherica* eroded much more rapidly than the ones with other species and the variation was also higher (Figure 9b).

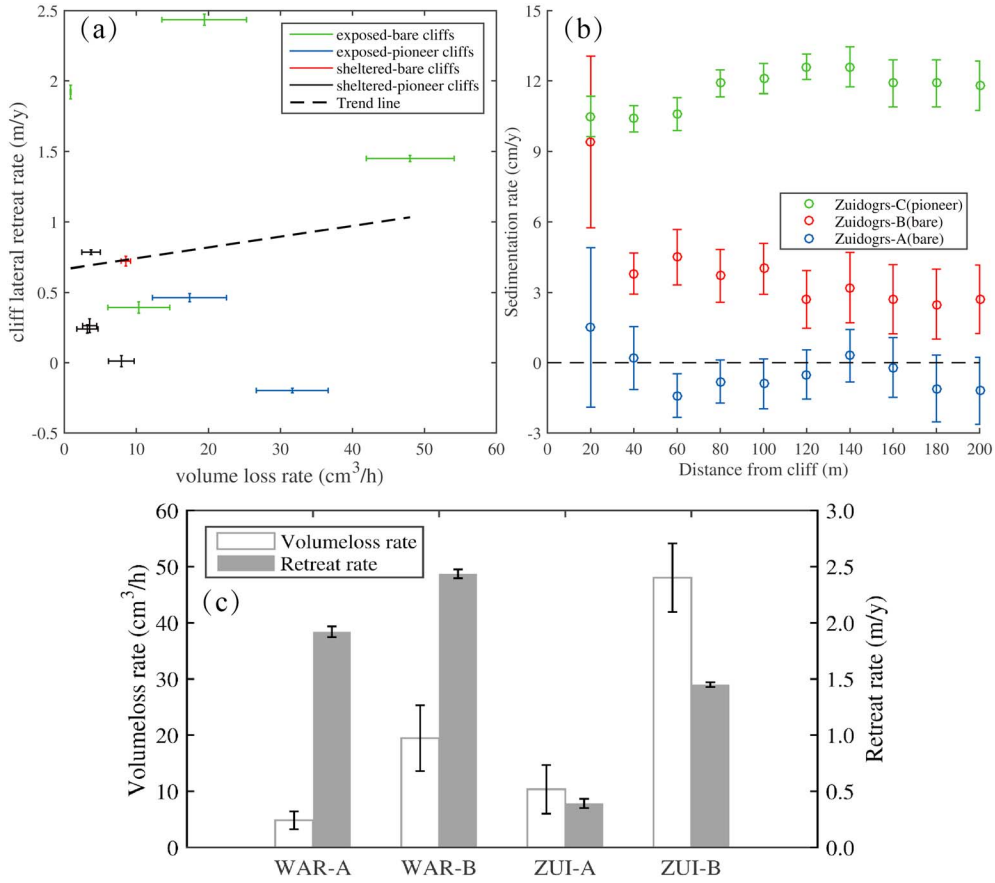


**Figure 8.** (a) Correlation between volume loss rates measured in wave tanks and cliff lateral retreat rates from GIS. Each data point represents the mean value ± standard error of volume loss rate (*x* axis) and lateral retreat rate (*y* axis) of the four cliff groups. (b) Net sedimentation rate on the mudflat of three stretches (A, B, and C) of exposed marsh site Zuidgors during 2012–2013. (c) The bar plots of volume loss rate (mean ± standard error, left *y* axis) in the wave tank experiment and lateral retreat rate (right *y* axis) at Waarde-A (WAR-A), Waarde-B (WAR-B), Zuidgors-A (ZUI-A), and Zuidgors-B stretches (ZUI-B).

## 4. Discussion

Previous studies identified wave force as the main driver of marsh edge destabilization and their subsequent collapse [*Tonelli et al.*, 2010]. This study uses a multiscale approach to understand how both extrinsic and intrinsic factors, which affect intensity of wave force and cliff stability, respectively, influence marsh edge erosion at different scales (Figure 10). At the large scale, the presence of pioneer vegetation and wind exposure strongly affected lateral retreat rate of cliffs. At the intermediate scale, foreshore morphology characters were linearly correlated to cliff retreat rate under comparable exposure and foreshore conditions. The factors at the large scale and the intermediate scale affect marsh edge erosion, through mitigating the wind waves (i.e., the external force). At the local scale, the erodibility of the sediment at the marsh edge played a large role in the local cliff retreat rate under identical hydrodynamic conditions. At the mesocosm scale, differences in cliff erodibility were determined by soil properties and belowground plant biomass. Briefly, at the two biggest scales, marsh edge erosion was governed by external forcing and related factors. Internal resistance of cliff affects marsh edge evolution at the local scale. Sediment and biological factors determined the erodibility of cliff and affect marsh edge erosion indirectly at the smallest scale. Thus, this study provides a comprehensive framework containing factors operating at nested scales, which may be used to predict the evolution of a marsh boundary. This hierarchical approach reveals that erosion of the salt marsh edge is a very complex process. Although we separated the factors according to the scales at which they influence marsh edge erosion, some factors were active across multiple scales. For example, wind exposure was linearly related to marsh edge erosion within exposed-bare and sheltered-pioneer groups (the intermediate scale). Within the exposed-bare group, the marsh edge of the more exposed stretches

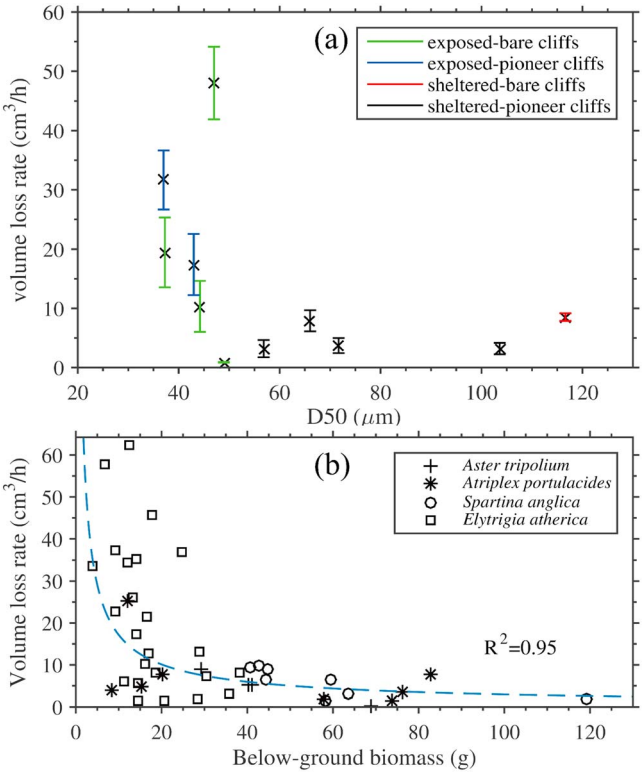


**Figure 9.** (a) The relationship between volume loss rate (mean ± standard error) and sediment grain size ($D_{50}$) of the 11 stretches. (b) The relationship between volume loss rate (mean ± standard error) and belowground biomass of 44 sediment cores collected under four species. The equation for the fitted curve: $y = 143.21x^{-0.83}$.

(Waarde A and B) retreated more rapidly than the sheltered ones (Zuidgors A and B). This indicates that wind exposure, the dominant external force, affected erosion rate not only at the large scale but also at the intermediate and local scales. This emphasizes the importance of relationships between different scales and the limitation of focusing the effect of factors at only one scale.

The relation between the wave power and marsh/seagrass edge erosion was quantified in previous studies [*Marani et al.*, 2011; *Rubegni et al.*, 2013]. In addition, wave energy is a function of effective fetch [*Young and Verhagen*, 1996a, 1996b], which is highly determined by the direction of wave propagation and the wind exposure. In the Westerschelde, the wave height and subsequent erosivity increased with exposure to the predominant wind direction (Figure 5). Here the two linear relations, i.e., the lateral erosion rate of the marsh edge against wind exposure (Figure 5b) and the wave height against wind exposure (Figure 6b), indicate that wind exposure reflects the extent at which the shoreline is exposed to the wind-induced hydrodynamic forces. Thus, our results linked the evolution of marsh edge with wind exposure, which was also linked with wind waves.

Our results clearly indicate that rates of bare cliff retreat are positively correlated with wind exposure and that cliffs with pioneer vegetation in front generally retreat more slowly than bare cliffs, rarely varying with wind exposure. It is important to note that the statistical correlation does not necessarily prove causality. Pioneer vegetation may be a surrogate for more benign abiotic conditions at the site, and demonstrating that pioneer vegetation cause the slow marsh edge erosion is arbitrary. As demonstrated at the Zuidgors site, the foreshore pioneer vegetation has grown for decades. The effect of ecosystem engineering provided by plants

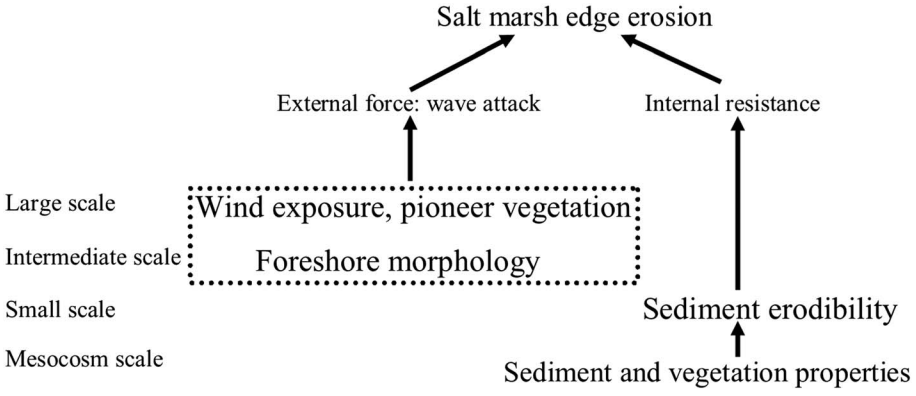


**Figure 10.** A schematic view of extrinsic and intrinsic factors affecting salt marsh edge erosion across different scales. The arrows indicate the flow of influence.

at the same time facilitates plant growth resulting in a positive feedback between plant growth, accretion and abiotic stress attenuation (i.e., hydrodynamic force [*van de Koppel et al.*, 2005; *Mudd et al.*, 2010; *van Wesenbeeck et al.*, 2008; *Wang and Temmerman*, 2013; *Ackerman and Okubo*, 1993; *Leonard and Luther*, 1995; *Koch and Gust*, 1999; *Bouma et al.*, 2005; *van Wesenbeeck et al.*, 2007; *Yang et al.*, 2011; *Schwarz et al.*, 2016]). Once the pioneer vegetation is established, the positive feedback between sedimentation and tussock growth can result in a buffer in front of the older marsh, further diminishing the wave forces and slowing down the lateral retreat rate of the salt marsh plateau [*van der Wal et al.*, 2008]. Our study indicates that that pioneer vegetation is associated with attenuating marsh edge erosion at the large scale and can be a sign of marsh accretion and propagation. Moreover, mudflats with adequate sediment supply can prograde seaward and accrete vertically, until a point where subsequent pioneer species establishment and colonization are possible [*Gunnell et al.*, 2013; *Hu et al.*, 2015], even in the presence of waves. The presence of pioneer vegetation might indicate a large sediment supply that favors bed accretion and subsequent colonization. This might be one reason that the marsh edge erosion rate is not linearly related to wind exposure for cliffs with pioneer vegetation. Thus, it is possible that there is a surplus of sediment that dominates the marsh edge dynamics and reduces the signal of wave erosion in the marshes with pioneer vegetation. It is promising to relate sediment availability with the presence of pioneer vegetation and marsh edge erosion in the future, and the relationship between sediment supply and pioneer vegetation is not addressed in this study.

The present study specifically highlights the importance of foreshore morphology to marsh boundary lateral erosion, which has rarely been addressed [i.e., *Mariotti and Fagherazzi*, 2013]. Once we zoom in at the intermediate scale, at which cliffs were grouped by wind exposure (exposed or sheltered) and pioneer condition (with or without pioneer vegetation in front of the cliff), foreshore morphology played an important role in the rate of cliff retreat. It is interesting to note that in each group, the correlated coefficients of the whole group were generally higher than that for the cliffs of one site in that group, except for the sheltered-pioneer group. This indicates that cliff retreat rate is better described by foreshore morphology at the intermediate scale than at a smaller scale. Channel width was significantly associated with cliff retreat rate, such that cliffs fronted by wider channels tended to retreat more rapidly. Waves caused by ships may aggravate marsh edge erosion [*Silinski et al.*, 2015]. Moreover, mudflat morphology, including mudflat width and mudflat slope, affected wave attenuation, which is determined by water depth [*van de Koppel et al.*, 2005; *Mariotti et al.*, 2010], and the cross-shore location of possible cliff formation is determined by the ratio of wave height to water depth [*Feagin et al.*, 2009]. However, it is remarkable that wind exposure was not related to cliff retreat rate at the intermediate scale ($p > 0.05$; Table 4) except for exposed-bare cliffs ($p < 0.001$). Despite similar wind exposure and pioneer vegetation condition, marsh edge erosion rate varied with wind exposure for exposed-bare cliffs. Consequently, marsh edge erosion at the intermediate scale was mainly affected by foreshore morphology, and wind exposure only played a role at exposed and unprotected sites.

The wave tank experiment could not capture mass wasting, which may be an important component of marsh edge retreat at the large scale. As observed in the field, the scale of collapsed sediment blocks is ~1 m, which is much larger than the scale of the surface erosion from the cores in the wave tank. This may have contributed to the lack of correlation between the marsh edge erosion rates in the field and the sediment erodibility measured in the mesocosm. However, once we zoomed in at the local scale, good agreement was found between the sediment erodibility measured in wave tanks and cliff lateral retreat rate when excluding the effect of extrinsic factors at the local scale (within one cliff group) (Figure 10). This result not only links sediment erodibility under identical wave conditions and in situ marsh edge erosion but also clarifies the scale at which sediment erodibility plays a role. However, because of the strong effect of extrinsic factors, cliff retreat rate was not correlated with sediment erodibility even within one marsh site.

Exerting both extrinsic and intrinsic influences, biological factors including pioneer vegetation and below-ground biomass played important roles in mediating marsh edge erosion at the extreme ends of the scale, the large and mesocosm scales. This indicates that biological measures can be widely applied in some salt marsh restoration. Our findings are highly relevant for the management and restoration of salt marshes, in that salt marsh restoration efforts should be adopted based on the aims and the scale of the specific project. Understanding to what extent, and at what scale, factors affect marsh edge erosion may help formulate effective management policies. For instance, since wind exposure affects marsh edge erosion at both large and intermediate scales, to protect the marsh edge of the whole estuary, artificial constructions or nature-

based solutions could be employed as shelters from wind-generated waves originating from the high-frequency directions (i.e., dikes at stretch C of site Waarde; Figure 1c). Artificial constructions can attenuate the wave erosivity and facilitate establishment of pioneer vegetation. Regarding nature-based solutions, the positive feedback between sedimentation and tussock growth results in a buffer at the front of marsh edge, which gradually slows down the erosion process [*van de Koppel et al.*, 2005; *van der Wal et al.*, 2008]. *Feagin et al.* [2009] found no effect of vegetation on surface erosion and marsh edge lateral erosion. On the contrary, our experimental results indicate that natural sediment erodibility is influenced by belowground biomass, which is strongly linked to species traits and sediment properties. Sediment samples containing growing plants with denser root systems were more resistant to wave attack, thus indicating a potential to retard the marsh edge erosion. Specific plants with dense root systems can be used as "binding agents" to modify sediment properties and enhance the stability of the marsh edge. Such local species can be transplanted to collapsed areas with high erodibility to reinforce the marsh edge. When implementing such measures, other aspects such as issues related to biodiversity and invasive species, including *Spartina anglica* [*Nehring and Hesse*, 2008], should also be considered to develop effective, safe, and practical nature-based measures for the protection of marshes.

## 5. Conclusions

This study fills a knowledge gap by identifying the scale-dependent factors affecting marsh edge erosion using a multiscale approach, which links cliff lateral retreat rate at the large scale to sediment erodibility at the local scale. Our findings contribute to providing a more holistic understanding of the role that extrinsic and intrinsic factors play on the retreat of the marsh edge. In conclusion, wind exposure and pioneer vegetation played an important role in cliff retreat at the large scale, foreshore morphology was partially related to cliff retreat at the intermediate scale, and soil and vegetation properties determined sediment erodibility at the local scale. Our findings also point to the importance of hydrodynamic and biogeomorphologic processes for the stability of foreshore environments and suggest that salt marsh regression is closely linked to the feedback between physical dynamics and the vegetation.

**Acknowledgments**

This work was jointly funded by the National Key Research and development program of China (2016YFC1201100), the BE-SAFE project (NWO-BwN, 850.13.011), the FAST project (EU FP7, 607131), the SKLEC research funding (2015KYYW03), and the Sino-Dutch Bilateral Exchange Scholarship program granted by Nuffic. We are indebted to Sil Nieuwhof, Jeroen van Dalen, Lennart van Ijzerloo, and Veronica Lo for developing the methodology to quantify sediment volume loss and are also grateful to Zhenchang Zhu, Zhigang Ma, and Isabella Kratzer for their kind assistance in the field work and to Annette Wielemaker for providing the location map. Thanks to the Editor and anonymous reviewers for their comments which much improved the manuscript. Data and scripts will be available at doi:10.4121/uuid:214b7b5f-84cc-4b16-8026-3b76463e128d. Authors declare no conflicts of interest.

## References

Ackerman, J., and A. Okubo (1993), Reduced mixing in a marine macrophyte canopy, *Funct. Ecol.*, 305–309.

Allen, J. (2002), Retreat rates of soft-sediment cliffs: The contribution from dated fishweirs and traps on Holocene coastal outcrops, *Proc. Geol. Assoc.*, *113*(1), 1–8.

Booij, N., R. Ris, and L. H. Holthuijsen (1999), A third-generation wave model for coastal regions: 1. Model description and validation, *J. Geophys. Res.*, *104*(C4), 7649–7666, doi:10.1029/98JC02622.

Bouma, T., M. De Vries, E. Low, G. Peralta, I. Tánczos, J. van de Koppel, and P. M. J. Herman (2005), Trade-offs related to ecosystem engineering: A case study on stiffness of emerging macrophytes, *Ecology*, *86*(8), 2187–2199.

Bouma, T. J., J. van Belzen, T. Balke, Z. Zhu, L. Airoldi, A. J. Blight, A. J. Davies, C. Galvan, S. J. Hawkins, and S. P. Hoggart (2014), Identifying knowledge gaps hampering application of intertidal habitats in coastal protection: Opportunities & steps to take, *Coast. Eng.*, *87*, 147–157.

Callaghan, D. P., T. J. Bouma, P. Klaassen, D. van der Wal, M. J. F. Stive, and P. M. J. Herman (2010), Hydrodynamic forcing on salt-marsh development: Distinguishing the relative importance of waves and tidal flows, estuarine, *Coast. Shelf Sci.*, *89*(1), 73–88, doi:10.1016/j.ecss.2010.05.013.

Clough, J. S., R. A. Park, and R. Fuller (2010), SLAMM 6 beta technical documentation, Waitsfield, VT.

Craft, C., J. Clough, J. Ehman, S. Joye, R. Park, S. Pennings, H. Guo, and M. Machmuller (2008), Forecasting the effects of accelerated sea-level rise on tidal marsh ecosystem services, *Front. Ecol. Environ.*, *7*(2), 73–78.

Doody, J. P. (2013), Coastal squeeze and managed realignment in southeast England, does it tell us anything about the future, *Ocean Coast. Manage.*, *79*, 34–41.

Fagherazzi, S., G. Mariotti, P. L. Wiberg, and K. J. McGlathery (2013), Marsh collapse does not require sea level rise, *Oceanography*, *26*, 70–77.

Feagin, R. A., S. M. Lozada-Bernard, T. M. Ravens, I. Möller, K. M. Yeager, and A. H. Baird (2009), Does vegetation prevent wave erosion of salt marsh edges, *Proc. Natl. Acad. Sci. U.S.A.*, *106*(25), 10,109–10,113, doi:10.1073/pnas.0901297106.

Fourqurean, J. W., C. M. Duarte, H. Kennedy, N. Marbà, M. Holmer, M. A. Mateo, E. T. Apostolaki, G. A. Kendrick, D. Krause-Jensen, and K. J. McGlathery (2012), Seagrass ecosystems as a globally significant carbon stock, *Nat. Geosci.*, *5*(7), 505–509.

Francalanci, S., M. Bendoni, M. Rinaldi, and L. Solari (2013), Ecomorphodynamic evolution of salt marshes: Experimental observations of bank retreat processes, *Geomorphology*, *195*, 53–65, doi:10.1016/j.geomorph.2013.04.026.

Gedan, K. B., B. Silliman, and M. Bertness (2009), Centuries of human-driven change in salt marsh ecosystems, *Mar. Sci.*, *1*.

Gunnell, J. R., A. B. Rodriguez, and B. A. McKee (2013), How a marsh is built from the bottom up, *Geology*, *41*(8), 859–862.

Hu, Z., Z. B. Wang, T. J. Zitman, M. J. Stive, and T. J. Bouma (2015), Predicting long-term and short-term tidal flat morphodynamics using a dynamic equilibrium theory, *J. Geophys. Res. Earth*, *120*, 1803–1823, doi:10.1002/2015JF003486.

Koch, E. W., and G. Gust (1999), Water flow in tide-and wave-dominated beds of the seagrass *Thalassia testudinum*, marine ecology, *Progr. Ser.*, *184*, 63–72.

Leonard, L. A., and M. E. Luther (1995), Flow hydrodynamics in tidal marsh canopies, *Limnol. Oceanogr.*, *40*(8), 1474–1484.

Manca, E., I. Caceres, J. M. Alsina, V. Stratigaki, I. Townend, and C. L. Amos (2012), Wave energy and wave-induced flow reduction by full-scale model *Posidonia oceanica* seagrass, *Cont. Shelf Res.*, *50-51*, 100–116, doi:10.1016/j.csr.2012.10.008.

Marani, M., A. D'Alpaos, S. Lanzoni, and M. Santalucia (2011), Understanding and predicting wave erosion of marsh edges, *Geophys. Res. Lett.*, *38*, L21401, doi:10.1029/2011GL048995.

Mariotti, G., and S. Fagherazzi (2010), A numerical model for the coupled long-term evolution of salt marshes and tidal flats, *J. Geophys. Res.*, *115*, F01004, doi:10.1029/2009JF001326.

Mariotti, G., and S. Fagherazzi (2013), Critical width of tidal flats triggers marsh collapse in the absence of sea-level rise, *Proc. Natl. Acad. Sci. U.S.A.*, *110*(14), 5353–5356, doi:10.1073/pnas.1219600110.

Mariotti, G., S. Fagherazzi, P. Wiberg, K. McGlathery, L. Carniello, and A. Defina (2010), Influence of storm surges and sea level on shallow tidal basin erosive processes, *J. Geophys. Res.*, *115*, C11012, doi:10.1029/2009JC005892.

Möller, I., et al. (2014), Wave attenuation over coastal salt marshes under storm surge conditions, *Nat. Geosci.*, *7*(10), 727–731, doi:10.1038/ngeo2251.

Mudd, S. M., A. D'Alpaos, and J. T. Morris (2010), How does vegetation affect sedimentation on tidal marshes? Investigating particle capture and hydrodynamic controls on biologically mediated sedimentation, *J. Geophys. Res.*, *115*, F03029, doi:10.1029/2009JF001566.

Nehring, S., and K. J. Hesse (2008), Invasive alien plants in marine protected areas: The *Spartina anglica* affair in the European Wadden Sea, *Biol. Invasions*, *10*(6), 937–950, doi:10.1007/s10530-008-9244-z.

Nieuwhof, S., P. M. Herman, N. Dankers, K. Troost, and D. van der Wal (2015), Remote sensing of epibenthic shellfish using synthetic aperture radar satellite imagery, *Remote Sens.*, *7*(4), 3710–3734.

Ris, R., L. Holthuijsen, and N. Booij (1999), A third-generation wave model for coastal regions: 2. Verification, *J. Geophys. Res.*, *104*(C4), 7667–7681, doi:10.1029/1998JC900123.

Rubegni, F., E. Franchi, and M. Lenzi (2013), Relationship between wind and seagrass meadows in a non-tidal eutrophic lagoon studied by a Wave Exposure Model (WEMo), *Mar. Pollut. Bull.*, *70*(1–2), 54–63, doi:10.1016/j.marpolbul.2013.02.012.

Schwarz, C., T. Ysebaert, W. Vandenbruwaene, S. Temmerman, L. Q. Zhang, and P. M. J. Herman (2016), On the potential of plant species invasion influencing bio-geomorphologic landscape formation in salt marshes, *Earth Surf. Process. Landforms*, *41*(14).

Schwimmer, R. A. (2001), Rates and processes of marsh shoreline erosion in Rehoboth Bay, Delaware, USA, *J. Coast. Res.*, 672–683.

Silinski, A., M. Heuner, J. Schoelynck, S. Puijalon, U. Schroder, E. Fuchs, P. Troch, T. J. Bouma, P. Meire, and S. Temmerman (2015), Effects of wind waves versus ship waves on tidal marsh plants: A flume study on different life stages of *Scirpus maritimus*, *PLoS One*, *10*(3), e0118687, doi:10.1371/journal.pone.0118687.

Solomon, S. (2007), *Climate Change 2007—The Physical Science Basis: Working Group I Contribution to the Fourth Assessment Report of the IPCC*, pp. 123–124, Cambridge Univ. Press, Cambridge, U. K.

Tonelli, M., S. Fagherazzi, and M. Petti (2010), Modeling wave impact on salt marsh boundaries, *J. Geophys. Res.*, *115*, C09028, doi:10.1029/2009JC006026.

van de Koppel, J., D. van der Wal, J. P. Bakker, and P. M. Herman (2005), Self-organization and vegetation collapse in salt marsh ecosystems, *Am. Nat.*, *165*(1), E1–E12.

van der Wal, D., A. Wielemaker-Van den Dool, and P. M. J. Herman (2008), Spatial patterns, rates and mechanisms of saltmarsh cycles (Westerschelde, The Netherlands), estuarine, *Coast. Shelf Sci.*, *76*(2), 357–368, doi:10.1016/j.ecss.2007.07.017.

van Wesenbeeck, B., J. van de Koppel, P. Herman, J. Bakker, and T. Bouma (2007), Biomechanical warfare in ecology; negative interactions between species by habitat modification, *Oikos*, *116*(5), 742–750.

van Wesenbeeck, B. K., J. van de Koppel, P. M. Herman, M. D. Bertness, D. van der Wal, J. P. Bakker, and T. J. Bouma (2008), Potential for sudden shifts in transient systems: Distinguishing between local and landscape-scale processes, *Ecosystems*, *11*(7), 1133–1141.

Wang, C., and S. Temmerman (2013), Does biogeomorphic feedback lead to abrupt shifts between alternative landscape states?: An empirical study on intertidal flats and marshes, *J. Geophys. Res. Earth*, *118*, 229–240, doi:10.1029/2012JF002474.

Wang, H., Z. Ge, L. Yuan, and L. Zhang (2014), Evaluation of the combined threat from sea-level rise and sedimentation reduction to the coastal wetlands in the Yangtze estuary, China, *Ecol. Eng.*, *71*, 346–354, doi:10.1016/j.ecoleng.2014.07.058.

Winn, P., R. Young, and A. Edwards (2003), Planning for the rising tides: The Humber estuary Shoreline Management Plan, *Sci. Total Environ.*, *314*, 13–30.

Yang, S. L., B. W. Shi, T. J. Bouma, T. Ysebaert, and X. X. Luo (2011), Wave attenuation at a salt marsh margin: A case study of an exposed coast on the Yangtze estuary, *Estuar. Coasts*, *35*(1), 169–182, doi:10.1007/s12237-011-9424-4.

Young, I., and L. Verhagen (1996a), The growth of fetch limited waves in water of finite depth. Part 1. Total energy and peak frequency, *Coast. Eng.*, *29*(1–2), 47–78.

Young, I., and L. Verhagen (1996b), The growth of fetch limited waves in water of finite depth. Part 2. Spectral evolution, *Coast. Eng.*, *29*(1–2), 79–99.